The Society of SCR Chromosome Research

Regular Article

Mitotic Chromosome Coating Spheres, MiCCS: Distinguished components of RNA molecules surrounding mitotic chromosomes in mammalian cells

Marin Chiba and Hideyuki Tanabe

Received: September 2, 2010 / Accepted: December 6, 2010

Abstract

Recently, RNA molecules in mammalian cells have been extensively studied, but their role in mitosis is not fully understood because of the mitotic repression of transcription, that is, the repression of transcripts from mitotic chromosomes. Several studies have identified the distribution and function of RNA molecules in mitosis; however, the relationships between RNA molecules and condensed chromosomes during mitosis have not been systematically studied. In this study, we investigated specific RNA molecules during mitosis and identified structural components that surround the chromosomes, called Mitotic Chromosome Coating Spheres (MiCCS), by using an in-cell deproteinization assay. Furthermore, we observed the unique distribution patterns of the RNA molecules—in terms of mitotic chromosomes, MiCCS, mitotic cytoplasm, and outer membranes of mitotic cells—by using a mitotic three-dimensional RNA fluorescent *in situ* hybridization (3D-RNA-FISH). These data provide us with a novel perspective of the relationships between RNA molecules and mitotic chromosomes.

Key words: RNA, mitosis, MiCCS, 3D-RNA-FISH

Marin Chiba

Department of Evolutionary Studies of Biosystems
School of Advanced Sciences
The Graduate University of Advanced Studies (SOKENDAI)
Shonan Village, Hayama, Kanagawa 240-0193, Japan

Research Fellowship for Young Scientists (DC2),
the Japan Society for Promotion of Science

Hideyuki Tanabe (✉)

Department of Evolutionary Studies of Biosystems
School of Advanced Sciences
The Graduate University of Advanced Studies (SOKENDAI)
Shonan Village, Hayama, Kanagawa 240-0193, Japan
E-mail: tanabe_hideyuki@soken.ac.jp
Phone: +81-46-858-1573, Fax: +81-46-858-1544

Introduction

Mitosis is characterized by the segregation of genomic and cellular information into two daughter cells. This event consists of the condensation of chromosomes, repression of RNA transcription, segregation of homologous chromosomes, and redistribution of nuclear proteins as well as numerous small molecules. These processes are highly organized and require the orchestrated dynamics of thousands of biological molecules in a short period. Proteins, on the one hand, have especially significant roles in maintaining cellular functions during mitosis. Despite the fact that many studies have focused on the identification and characterization of mitotic proteins, there are still many unanswered questions regarding the mitosis of mammalian cells (Lewis and Laemmli 1982; Gasser *et al.* 1986; van Holde 1988; Uchiyama *et al.* 2005). RNA molecules, on the other hand, have recently become a focus of attention because both coding and non-coding RNA molecules play significant roles in cellular metabolism and structure during the cell cycle. Previously, in order to investigate how degree of RNA molecules is synthesized during mitosis, biochemical assays using autoradiographic techniques with radiolabeled-uridine have been performed in amoeba cells (Goldstein and Ko 1978) and mammalian cells (Konrad 1963; King and Barnhisel 1967). These studies revealed that RNA synthesis has fallen drastically during mitosis.

It has been considered that transcription is actively ongoing during interphase; however, it is repressed from prophase to telophase during mitosis (reviewed by Gottesfeld and Forbes 1997). This "mitotic repression of transcription" is the result of the three following biological processes: 1) chromosomal condensation leading to the physical inaccessibility of transcription factors and RNA polymerases to the DNA (Bradbury *et al.* 1974; Uemura *et al.* 1987; Hirano and Mitchison 1991; Chen *et al.* 2005) ; 2) inactivation of transcriptional factors and their associated machinery by phosphorylation (Prescott 1964; Gottesfeld *et al.* 1994; Dahmus 1995; Segil *et al.* 1996); and 3) activation of repressor genes as general repressor proteins (Strunnikov 2005; Chuang *et al.* 1994). Although the mitotic repression of transcription was identified over four decades ago, the biological mechanisms underlying the global repression of transcription during mitosis have yet to be fully elucidated, and the RNA molecules present during mitosis may be responsible for important cellular functions.

In this study, first we revealed the distribution of global RNA molecules during mitosis using an in-cell deproteinization assay. We identified structural components that surround the chromosomes, called "Mitotic Chromosome Coating Spheres (MiCCS)". Second, we verified the presence of MiCCS in human tumor cell lines and mammalian cells derived from several species to determine whether MiCCS are a common feature among mammalian mitotic cells. Third, we observed the distribution of the RNA molecules on the metaphase chromosome spreads. Furthermore, we demonstrated the distribution patterns of specific RNA molecules in mitotic cells using a mitotic three-dimensional RNA fluorescent *in situ* hybridization (3D-RNA-FISH) technique.

Materials and methods

Cell culture and preparation of slides

Six cell lines, HeLa (JCRB9004; human epithelial carcinoma cell lines), TIG-1-20 (JCRB0501; human fetal lung fibroblasts), T98G (JCRB9041; human glioblastoma multiform tumor cell lines), BHK-21 (C-13) (JCRB9020; Syrian hamster *Mesocricetus auratus* kidney fibroblast-like cells), Indian Muntjac (JCRB9100; Indian muntjac *Muntiacus muntjak* skin fibroblasts), and Vero (JCRB0111; African green monkey *Cercopithecus aethiops* kidney epithelial-like cells), were provided by the JCRB/HSRRB cell bank. The detailed characteristics of each cell line and standard culturing procedures can be found on the JCRB/HSRRB website (http://cellbank.nibio.go.jp/index.html). For the preparation of slides, 0.25% trypsin (Gibco) and 0.02% EDTA in phosphate-buffered saline (PBS pH 7.4; Gibco: 70011; 1.06mM potassium phosphate monobasic, 155.2mM sodium chloride, and 2.97mM sodium phosphate dibasic) were used to remove the confluent cells from plastic culture dishes, and collected cells (0.5 × 105 cells per slide) were placed on glass coverslips (24 × 60 mm; Matsunami) in a 4-well slide chamber (Nunc). In order to retain the cells' three-dimensional (3D) morphology, the cells were fixed according to the method of Solovei *et al.* (2002a). Briefly, the cells were grown for 48 h to obtain mitotic cells, harvested with approximately 60% confluent, and washed in PBS. Then, the cells were fixed in 4% paraformaldehyde (PFA) in PBS for 10 min, and washed twice in PBS for 10 min. These slides were then ready to use for fluorescent staining and successive assays, and were stored at 4°C in 1× PBS until use.

For the preparation of metaphase spreads, standard cytogenetic procedures were applied according to the methods described by Tanabe *et al.* (2000). Briefly, cells were cultured in medium containing 0.04 μg/mL colcemid (KaryoMAX Colcemid Solution; Gibco) for 2 h, exposed to a hypotonic solution (0.2% trisodium citrate and 0.06 mol/L potassium chloride) for 22 min, and fixed with Carnoy's fixative (methanol:acetic acid, 3:1 (v/v)). A cell suspension was dropped onto a glass slide (20 μL per spot) and air-dried by using HANABI apparatus (ADStec) to make good quality spreads, and the slides were stored in sealing bags at -20°C until use.

In-cell deproteinization assay

For the in-cell deproteinization assay, the cell membranes were gently permeabilized, consequently, cytoplasmic protein was partly washed out and nuclear protein was weakly deproteinized, but intracellular structural components such as RNA-protein complex were retained. After PFA fixation, the cells were permeabilized using 0.5% Triton X-100 and 0.5% saponin in PBS for 10 min, followed by incubation in 20% glycerol in PBS for at least 30 min. The slides were then subjected to repeated freeze/thaw cycles in liquid nitrogen. The slides were subsequently treated in 0.1 N HCl for 10 min, and refixed in 1% PFA in PBS for 10 min, washed in PBS and 2×SSC (0.3M sodium chloride and 0.03M sodium citrate, made from UltraPure™ 20×SSC; Invitrogen; Cat No: 15557-044), incubated in 50% formamide in 2× SSC (pH 7.0), and stored at 4°C until use. Care was taken to avoid drying the cells during all of the procedures (Solovei *et al.* 2002b).

RNA/DNA fluorescent staining

For RNA and DNA fluorescent staining, we used RNA specific dye, SYTO RNASelect (Molecular Probes) for RNA and TOPRO-3 (Molecular Probes) for DNA on PFA-fixed and Carnoy-fixed slides of each cell line, respectively, according to the manufacturer's instructions. SYTO RNASelect enables to stain total RNA molecules in the live and fixed cells (Haugland 2005; Li *et al.* 2006; Santangelo *et al.* 2006; Rhee and Bao 2009). After staining, the slides were mounted with VECTASHIELD (Vector) to proceed image acquisition by confocal microscopy.

In-cell RNase Assay

For the in-cell RNase assay, after washing in 2× SSC, the slides were treated in an RNase A (100 μg/mL) solution (Sigma) at 37°C for 1 h, washed in 2× SSC, and mounted with VECTASHIELD after RNA/DNA fluorescent staining for microscopy.

Preparation of probes and PCR labeling

We selected the following RNA molecules for the 3D-RNA-FISH analysis: 5S rRNA, 18S rRNA, actin, gamma 1 (ACTG-1), and protein regulator of cytokinesis 1 (PRC1). These RNA molecules were known to exist at a quantity that could be easily observed within the cells. In order to verify the distribution of these RNA molecules on the slides, normal human fetal lung fibroblast TIG-1-20 cells were used. Total RNA fractions were collected from TIG-1-20 cell cultures by using an RNeasy Mini Kit (Qiagen) according to the manufacturer's instructions. To generate the cDNA probes, polymerase chain reaction (PCR) was performed with 35 cycles of 94°C for 1 min, 60°C for 2 min, and 72°C for 2 min, and a final step of 72°C for 10 min. Total RNA fractions were used as the PCR template, and the products were labeled with digoxigenin-11-dUTP (Roche) using labeled PCR amplification. Partial sequencing analysis using an ABI PRISM 3130 was performed for verification. The forward and reverse primers of each gene used in this study are shown in Table 1, which were obtained by custom order for Invitrogen Life Technologies Japan Ltd.

Mitotic 3D-RNA-FISH

Each amplified labeled cDNA probe was dissolved in a hybridization solution (50% formamide and 10% dextran sulfate in 2×SSC) at approximately 10 µg/mL. Heat-denaturation was performed at 80°C for 6 min, and the probes were then chilled on ice for 1 min. Denatured probes were promptly applied onto slides prepared for the in-cell deproteinization assay. Slides were hybridized at 37°C under humid conditions for more than 20 h. After hybridization, the slides were washed three times in 50% formamide in 2×SSC at 37°C for 5 min, and then washed twice in 2×SSC at room temperature for 3 min. The immunofluorescent detection of specific probes hybridized with complementary RNA molecules was performed by a series of incubations at 37°C for 50 min in 5% bovine serum albumin (BSA; Sigma) in 4×SSC plus 0.2% Tween-20 with a rabbit anti-digoxigenin antibody (Sigma) as the first layer and a goat anti-rabbit-Cy3 conjugated antibody (Amersham Pharmacia Biotech) as the second layer. Counterstaining for RNA and DNA on cells was performed using SYTO RNASelect and TOPRO-3, respectively. The slides were mounted with VECTASHIELD for microscopy.

Table 1. PCR primers for the preparation of 3D-RNA-FISH probes

Target RNA	Name	Primers	Product Size (base)
5S rRNA	5s-F	5′-acggccataccaccctgaacg-3′	108
	5s-R	5′-agcacccggtattcccaggc-3′	(5–112)
18S rRNA	18s-F	5′-agtacgcacggccggtacag-3′	572
	18s-R	5′-gaattaccgcggctgctggc-3′	(61–632)
ACTG-1	ACTG1-F	5′-tcctgggtatggaatcttgc-3′	854
	ACTG1-R	5′-agtaacagcccacggtgttc-3′	(871–1724)
PRC1	PRC1-F	5′-gcgtactcaaatccgagagc-3′	784
	PRC1-R	5′-actattggccgtagcattgg-3′	(1–784)

ACTG-1, actin, gamma 1; PRC1, protein regulator of cytokinesis 1.

Confocal microscopy and image acquisition

Cells were scanned with an axial distance of 200 nm using a confocal laser scanning microscope (LSM 510 META; Carl Zeiss Co., Ltd.) equipped with a 63×/1.4 Plan-Apochromat objective lens and 3 lasers with multi-argon (458/477/488/514 nm), helium-neon 1 (543nm), and helium-neon 2 (633nm). For each optical section, the images were recorded sequentially for two or three fluorochromes (FITC, Cy3, and Cy5). Image stacks with 512 × 512 pixels in each channel were used for subsequent image analyses with the LSM5 browser.

Results

Localization of RNA molecules during mitosis in Vero cells

We first carried out the in-cell RNase assay to determine whether the SYTO RNASelect signals reflected the presence of not DNA but RNA molecules during interphase and mitosis. During interphase, SYTO RNASelect signals were completely lost from the nucleolus and cytoplasm after RNase treatment. Similarly, during mitosis, no signal was observed on the mitotic chromosomes as well as cytoplasm after RNase treatment (Fig. 1). Therefore, the in-cell RNase assay confirmed that SYTO RNASelect signals were derived from RNA molecules.

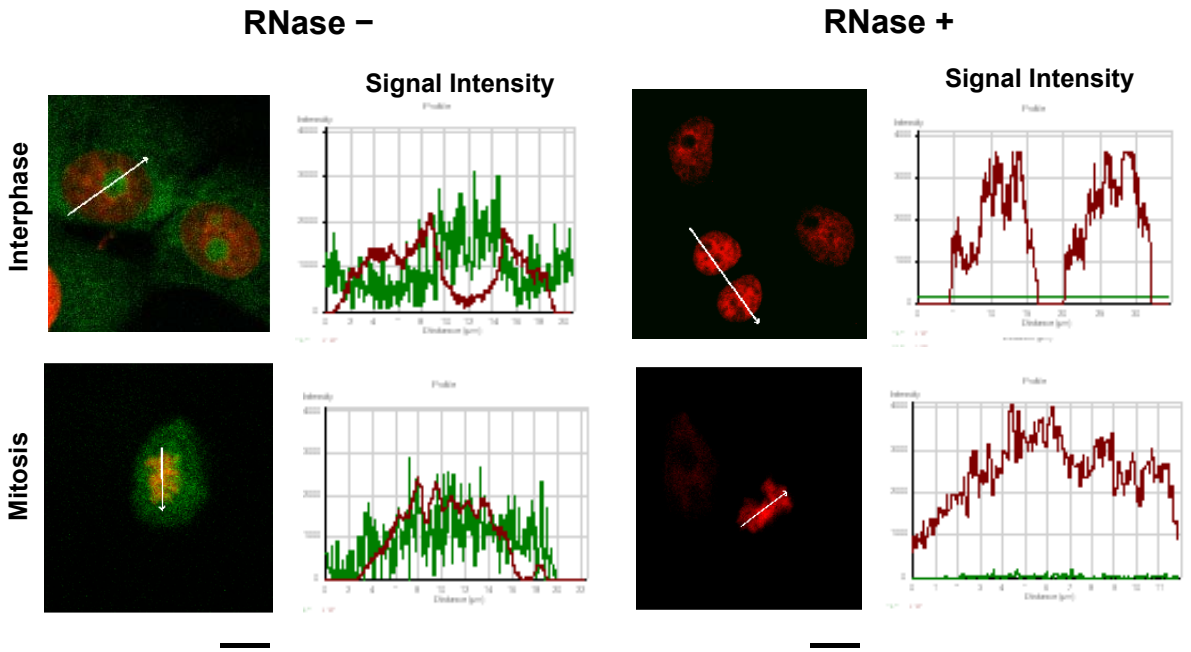

Figure 1 SYTO RNASelect staining represents in green color and DNA counterstaining with TOPRO-3 represents in red color in Vero cells. Different signal intensity patterns derived from SYTO RNASelect staining for RNase A-treated cells (two right columns) and non-treated cells (two left columns). The second and fourth columns show the signal intensities taken along a line (shown as a white arrow in the adjacent image). The top row shows images of interphase cells and the bottom row shows images of mitotic cells. The bars represent 10 µm.

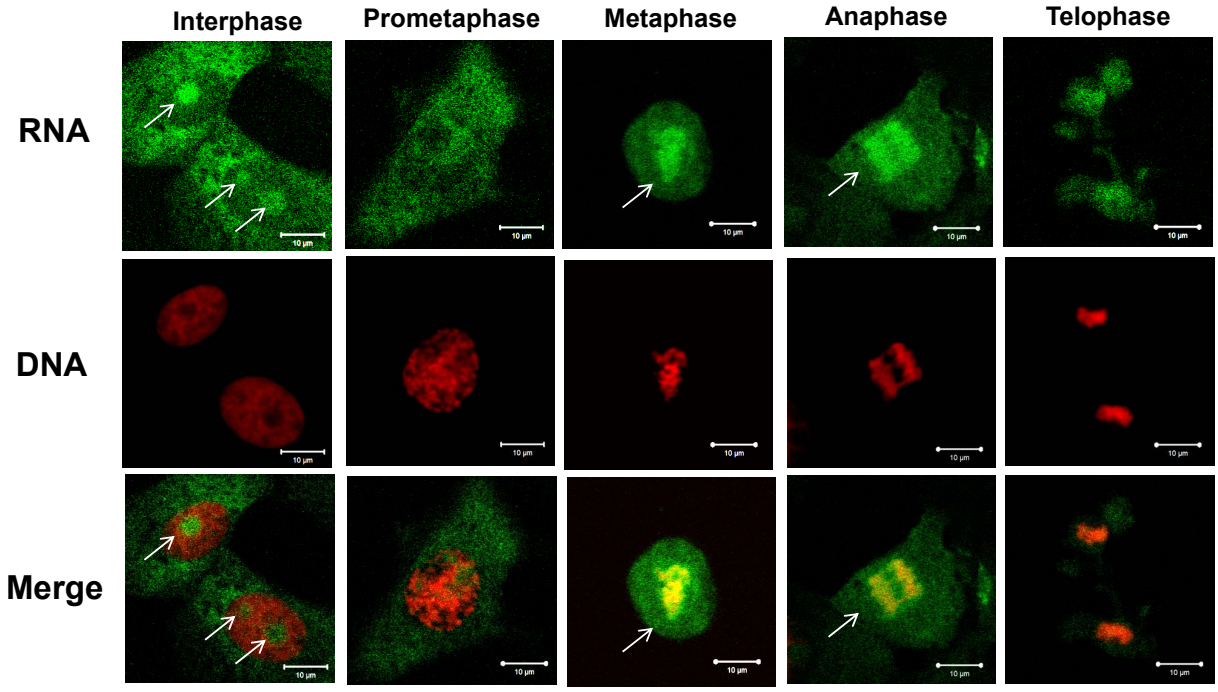

Figure 2 Distribution patterns of RNA molecules during interphase and mitosis in Vero cells. Each column represents the typical appearance of cells in the defined cell cycle period. The upper row shows the distribution patterns of the RNA molecules stained by SYTO RNASelect. The middle row shows DNA counterstaining with TOPRO-3, and the lower row are the merged images of the upper and middle rows. White arrows indicate the nucleolus in the interphase and the diffuse signals surrounding the chromosomes in the metaphase and anaphase. The bars represent 10 µm.

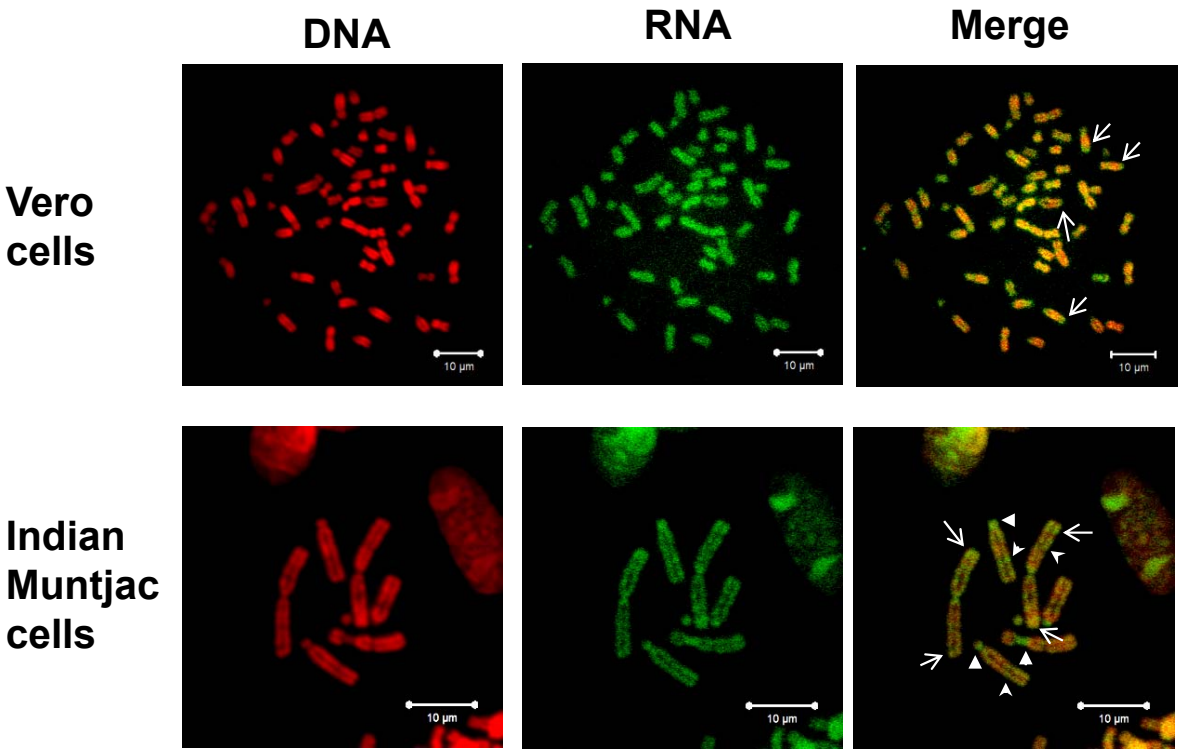

Figure 3 Metaphase chromosome spreads of Vero cells (top row) and Indian Muntjac cells (bottom row) stained by SYTO RNASelect (green) and TOPRO-3 (red). Merged images of RNA and DNA staining are shown in the third column. Large white arrows indicate the subtelomeric strong signals in Vero cells and Indian Muntjac cells, middle arrowheads indicate the centromeric signals and small arrowheads indicate the interstitial signals in Indian Muntjac cells. The bars represent 10 µm.

In order to investigate the distribution of RNA molecules during interphase and mitosis, we performed RNA and DNA fluorescent staining on Vero cells after PFA fixation. In the interphase cells, the RNA signals from SYTO RNASelect were clearly observed on the nucleolus and in the cytoplasm (Fig. 2, indicated by arrows). As the cell cycle proceeded and the cells entered into mitosis, the RNA signals on the nucleolus began to disappear and started to concentrate on the mitotic chromosomes. In the metaphase, the strong RNA signals were detected on the chromosomes and diffuse signals were widely observed in the cytoplasm. In the anaphase, as the mitotic chromosomes segregated, the RNA signals were still strongly detected on the chromosomes and in the cytoplasm. In the telophase, the RNA signals were almost lost but still retained on the mitotic chromosomes (Fig. 2).

Distribution of RNA molecules on the mitotic chromosomes

To further investigate the distribution of RNA molecules during mitosis, especially on the mitotic chromosomes, we prepared metaphase spreads and performed RNA and DNA fluorescent staining on Vero cells and Indian Muntjac cells (Fig. 3). Stronger RNA signals were observed on the specific chromosomal regions; subtelomeric regions in Vero cells and subtelomeric, centromeric, and interstitial regions in Indian Muntjac cells (Fig. 3, indicated by arrows and arrowheads). Dual color staining of RNA and DNA showed remarkable banding patterns on the mitotic chromosomes, but these patterns were distinct from previously reported banding patterns such as Q-/G-/Replication-banding patterns (Green and Bahr 1975; Ved Brat *et al.* 1979). These results suggested that the ratio of RNA/DNA varied among the chromosomal regions and the staining pattern did not reflect the DNA composite-like G-/R-banding patterns.

Mitotic chromosome coating spheres (MiCCS)

To verify the cellular structures composed of RNA molecules observed during mitosis in Vero cells, we performed the in-cell deproteinization assay. We observed the diffuse RNA signals widely in the cytoplasm during the metaphase to anaphase (Fig. 2, indicated by arrows). These structural components were obscure since they were masked by free RNA molecules in the cytoplasm. In order to remove the free RNA molecules in interphase and mitotic cells, but to maintain the structural components within the cells, we gently permeabilized the cell membranes and weakly deproteinized the cellular proteins. After permeabilization with 0.5% Triton X-100 in PBS and equilibration in 20% glycerol in PBS, we observed granule-like particle RNA signals with SYTO RNASelect staining (Fig. 4, indicated by arrowheads). These granule-like signals were increased and enhanced after the freeze-thaw process by liquid nitrogen (Fig. 4, indicated by arrows). Furthermore, these granule-like signals were disappeared after the cells were treated with 0.1N HCl but the RNA signals on the mitotic chromosomes were slightly enhanced. We found the RNA signals enhanced again not only in the mitotic cells but also in the interphase cells followed by incubation in 50% formamide in 2×SSC

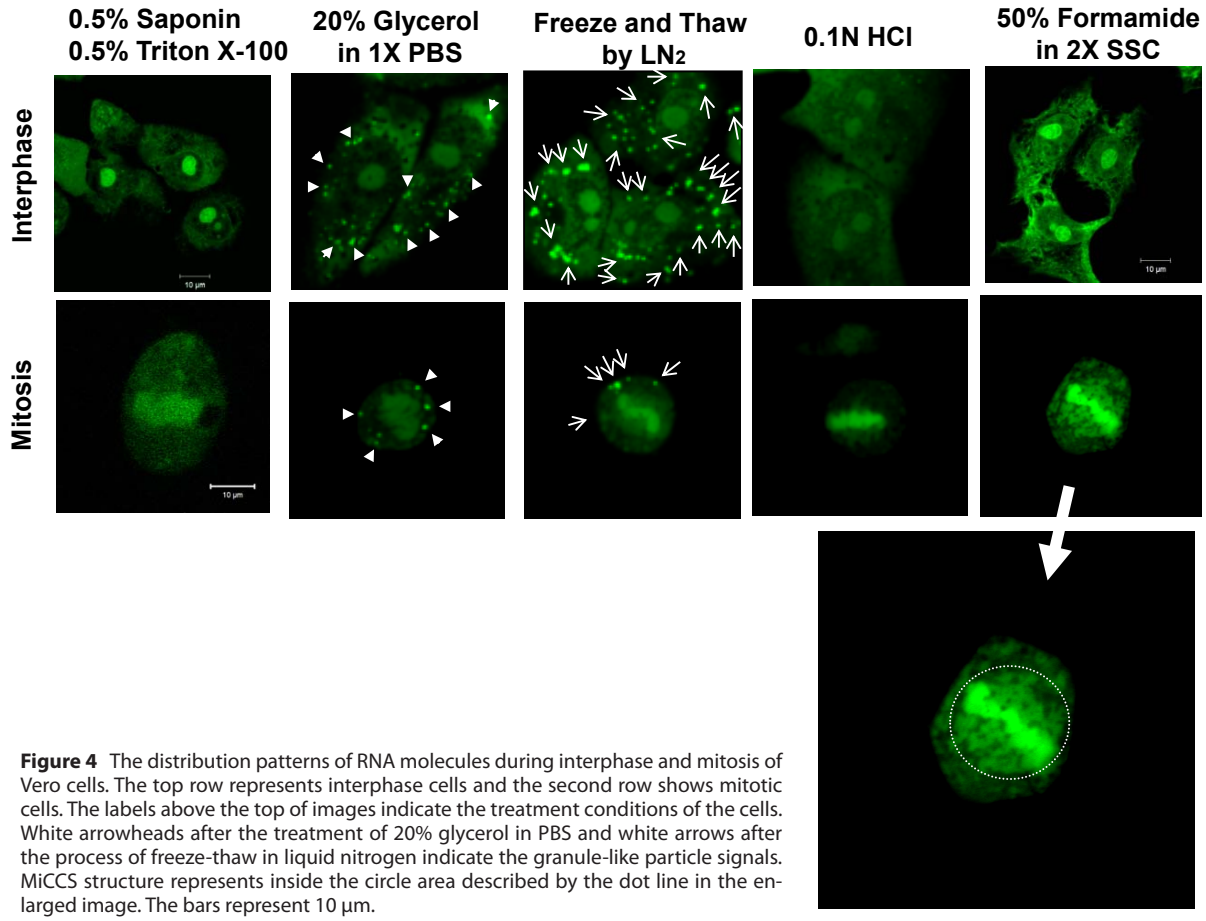

Figure 4 The distribution patterns of RNA molecules during interphase and mitosis of Vero cells. The top row represents interphase cells and the second row shows mitotic cells. The labels above the top of images indicate the treatment conditions of the cells. White arrowheads after the treatment of 20% glycerol in PBS and white arrows after the process of freeze-thaw in liquid nitrogen indicate the granule-like particle signals. MiCCS structure represents inside the circle area described by the dot line in the enlarged image. The bars represent 10 μm.

(Fig. 4). The RNA signals detected in 50% formamide in 2×SSC were reflected the richness of the RNA molecules after deproteinization in relation to cellular structures composed of RNA molecules in the interphase and mitotic cells. In particular, in the mitotic cells the higher-order structures were distinguished as components surrounding the condensed mitotic chromosomes in Vero cells (Fig. 4, indicated by the dot line). These structures, composed of full RNA molecules coating whole mitotic chromosomes, were mostly observed in the metaphase to anaphase in the mitotic cells. We called these higher-order RNA-rich structures "Mitotic Chromosome Coating Spheres (MiCCS) ". Three dimensional reconstructed images built from scanned image stacks by confocal microscopy revealed covering mitotic chromosomes by MiCCS structures in the metaphase cells (Fig. 5).

Comparison of MiCCS among mammalian cells

In order to compare the MiCCS structures observed in the mitotic Vero cells with other cells, we analyzed the following cell lines: HeLa, TIG-1-20, T98G, BHK-21 (C13), and Indian Muntjac (Fig. 5). In the human cells, HeLa, TIG-1-20, and T98G, we observed MiCCS after the in-cell deproteinization assay; however, the signal patterns were slightly different in these cell types, particularly in the T98G cells. This suggested that the MiCCS staining pattern depends on the cell types. Moreover, for the other mammalian cells, BHK-21 and Indian Muntjac cells, the MiCCS structures were quite similar to those observed in the other cells, although MiCCS structures were less pronounced than those of Vero cells. These results suggested that the MiCCS structures were commonly observed not only in primary cells but also in cancer cell lines, and in at least three different mammalian species other than humans. The degree of staining and the morphology of MiCCS varied among the cell lines and those were depending on the numbers of the highly organized mitotic RNA molecules surrounding the mitotic chromosomes.

Gradient patterning of RNA molecules determined by mitotic 3D-RNA-FISH

We applied 3D-RNA-FISH to TIG-1-20 cells in order to further characterize the distribution of the following RNA molecules during interphase and mitosis: 5S rRNA, 18S rRNA, ACTG-1, and PRC1 (Fig. 6).

5S rRNA and 18S rRNA

In the interphase cells, 3D-RNA-FISH signals for 5S rRNA were detected in the cytoplasm and nucleus, particularly in the nucleolus. In the mitotic cells, the signals for 5S rRNA were distributed mostly in the cytoplasm but in the chromosomal regions with less intensities. The distributed signal intensities of the mitotic cytoplasm were approximately twice higher than those of the chromosomal regions (Fig. 6). In contrast, in the interphase cells the

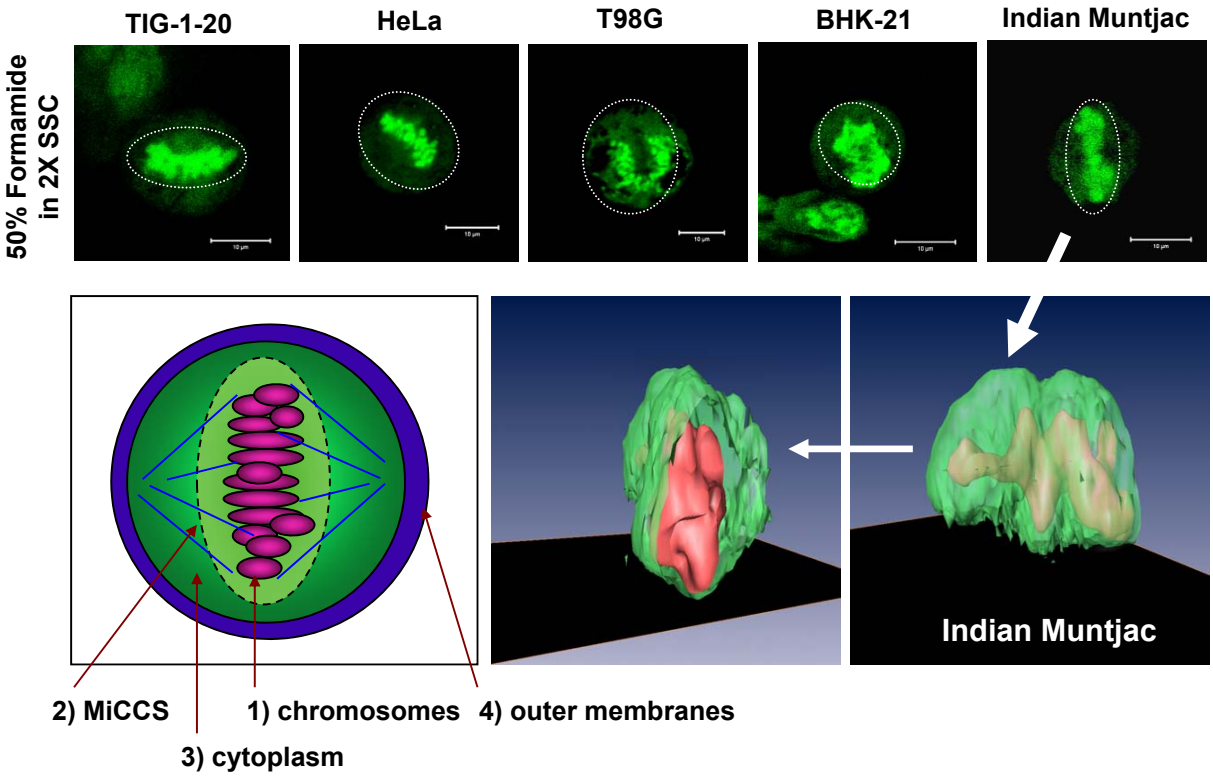

Figure 5 The top row shows MiCCS structures observed after the treatment of 50% formamide in 2xSSC conditions in HeLa, TIG-1-20, T98G, BHK-21, and Indian Muntjac cells. MiCCS structures represent inside the circle area described by the dot line in each mage. 3D-reconstructed images from the Indian Muntjac cell with MiCCS structure were illustrated in the center (partially turned up the MiCCS) and in the right side at the bottom row. The model image is shown in the left side at the bottom row indicating the four representative localization patterns of RNA molecules.

signals for 18S rRNA were observed in the cytoplasm but not in the nucleus. In the mitotic cells, however, the signals for 18S rRNA were mostly concentrated at inside the outer cell membrane and few signals were detected adjacent to or inside the chromosomal regions (Fig. 6).

ACTG-1 and PRC1

We arbitrarily selected ACTG, as a major component of the cytoskeleton, and PRC1, a protein regulator of cytokinesis, for use as probes by 3D-RNA-FISH. In the interphase cells, the signals for ACTG were observed throughout the cytoplasm and in the nucleus and nucleolus. In the mitotic cells, the signals for ACTG were distributed mainly in the cytoplasm and observed as punctuated foci rather than diffusive staining on the cytoplasm. Interestingly, some signals for ACTG were located inside and adjacent to the chromosomal regions (Fig. 6, indicated by arrows). In contrast, in the interphase cells the signals for PRC1 were hardly detected in the nucleus and cytoplasm, with very less intensities compared with those for ACTG. In the mitotic cells, the signals for PRC1 were distributed in the cytoplasm and observed as larger punctuated foci. The localization patterns for PRC1 in the mitotic cells were similar to those patterns for ACTG but the signal intensities for PRC1 were much less than those for ACTG (Fig.6).

Discussion

RNA molecules in mitosis

Various studies related to the distribution and functions of RNA molecules during mitosis in mammalian cells have been performed over the years (Konrad 1963; King and Barnhisel 1967; Goldstein 1976; Goldstein and Ko 1978); however, only a few studies have systematically analyzed the distribution and characteristics of RNA molecules and their relationships with cellular components in mitotic cells (Gottesfeld and Forbes 1997).

In this study, we demonstrated that the RNA molecules were distributed not only in the mitotic cytoplasm but also in the mitotic chromosomal regions with systematical verification throughout the mitosis; when cells enter into mitosis, chromosomal condensation is initiated simultaneously with the disassembly of the nucleolus and other cellular compartments. This is in consistent with our observation that the RNA signals on the nucleolus began to disappear and started to concentrate on the mitotic chromosomes (Fig. 2). As chromosomal condensation continues, the RNA molecules shift towards the chromosomal regions during the prometaphase to

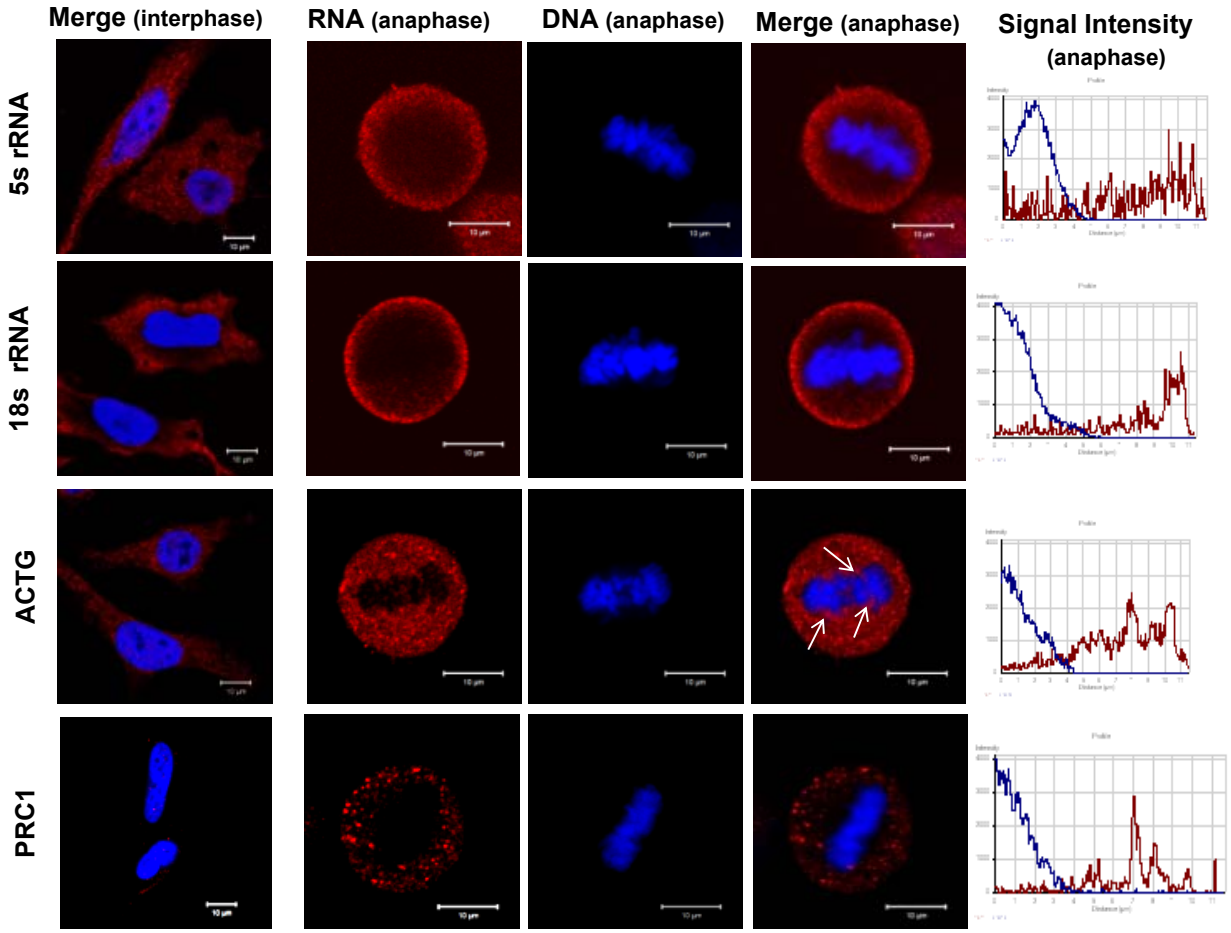

Figure 6 Localization patterns of RNA molecules for 5S rRNA, 18S rRNA, ACTG, and PRC1 by 3D-RNA-FISH during the interphase and anaphase of mitosis in TIG-1-20 cells. White arrows indicate the RNA signals adjacent to the chromosomal regions. Signal intensities in the anaphase taken along near the center to peripheral region were shown in the right column.

metaphase, which is confirmed by our observation that the strong RNA signals were deposited onto the specific chromosomal regions at centromeres, telomeres, and interstitial chromosomal regions (Fig. 3). We found also there are still existing diffusive widely signals in the mitotic cytoplasm during the metaphase to anaphase. This prompted us to examine the in-cell deproteinization assay. After the segregation of chromosomes in the anaphase, the RNA signals were still strongly detected on the chromosomes and in the cytoplasm. In the telophase, the RNA signals were almost lost on the mitotic chromosomes but still remained compared to those signals in the early G1 phase. In the early G1 phase, the RNA molecules would play crucial roles in the formation of the cellular structures of newly divided daughter cells. During the mitosis of mammalian cells, mitotic repression mechanisms halt the transcription of the RNA molecules, therefore, solely stored RNA molecules, which are transcribed until G2 phase of parental cells, would be providing for building cellular structures due to the dependent on the formation and deformation of cellular structures during the cell division. Accordingly, RNA molecules localized in cytoplasm and mitotic chromosomes during the telophase to early G1 phase would supply to synthesize ribosome machineries and consequently to form cellular organelles such as nucleus, Golgi apparatus, or scaffolding cytoskeleton structures and other proteins. The relationships between the localization patterns of RNA molecules and other functional proteins in the mitotic chromosomes remain to be determined; further studies are necessary to reveal these relationships in mitotic chromosomes.

Previously, RNA-FISH analysis showed that the telomeric repeat containing RNA molecules located at the telomeric repeats were present at the mitotic chromosomes in the human lung fibroblasts cells (Azzalin *et al*. 2007). In addition, other studies demonstrated that RNase treatment of mitotic cells dramatically affected the formation of kinetochores. Wong *et al*. (2007) inferred that the localization of the RNA molecules in centromeric satellite regions was essential for the formation of an integral component of the kinetochore. In addition, we showed the distribution of RNA molecules on the specific chromosomal regions. For example, in Indian Muntjak cells, bright RNA signals on the subtelomeric regions of chromosome 1p and the centromeric regions of chromosome 2 and X are distinct from the Q/G-banding patterns (Fig.3; indicated by arrowheads and arrows). This implies that it has been reflected the gene-dense regions where the numbers of the RNA molecules are maintained. These RNA molecules would be necessary to supply in the telophase or early G1 phase before the transcription is initiated.

Mitotic chromosome coating spheres (MiCCS)

In the cytoplasm of mitotic cells, previous studies reported the presence of RNA-containing particles during mitosis in rat liver cells (Kleinfeld and von Haam 1959). In addition, RNA molecules functioning as part of the nucleolar machinery and processes localize not only to the perichromosomal regions but also to the mitotic spindles (Mello *et al*. 1999; Mello *et al*. 2001; reviewed by van Hooser *et al*. 2005). In the metaphase, we demonstrated that the higher-order structures were composed of large numbers of RNA molecules, called MiCCS. Such MiCCS structures were observed until anaphase, the initiation of chromosomal segregation, and disappeared in the early G1 phase. MiCCS are commonly observed in mammalian mitotic cells, but they displayed cell- and species-specific distribution patterns and densities (Fig. 5). In mitotic cells, higher-order structural components are maintained to sustain essential cellular functions. Failure to maintain these components would lead to defects in chromosomal segregation, cytoplasmic segregation, and daughter cell formation, resulting in the induction of apoptosis or chromosome loss observed in cancer cells.

In this study, we also demonstrated that the structure of the MiCCS was relatively disorganized in HeLa cells and severely disorganized in T98G cells, compared to Vero, TIG-1-20, BHK-21, and Indian Muntjac cells (Fig. 5). Chromosomal segregation and behavior are highly dependent on the centromere protein families and kinetochore components of mitotic cells, and these proteins are evolutionary conserved in function throughout mammalian cells (reviewed by Kitagawa and Hieter 2001; Wieland *et al*. 2004). Therefore, the highly organized structure of MiCCS surrounding the mitotic chromosomes was considered to be related to the factors important for chromosomal segregation such as centromeric protein families, kinetochores components, microtubule-organizing center (MTOCs), or mitotic spindle apparatus. In addition, we demonstrated that MiCCS were observed in all of the mammalian cells examined, and were located adjacent to the mitotic chromosomes despite the presence of cell-specific differences in their distribution.

The 3D-RNA-FISH experiments in the mitotic cells revealed that the RNA molecules were distributed in a gradient rather than with distinct positioning at specific cellular structures (Fig. 6). In interphase cells, as the cellular morphology is flat-shape in culture, the cellular compartments are highly partitioned by the cellular organelles such as the nucleus, Golgi apparatus, endoplasmic reticulum, and mitochondria. Conversely, mitotic cells are nearly spherical-shape, and the cellular organelles are disassembled during mitosis (reviewed by Strunnikov 2005; reviewed by Güttinger *et al*. 2009). To efficiently produce the proteins required for cell division during mitosis, the RNA molecules are considered to be specifically distributed inside the whole cellular compartments. In this study, we demonstrated that there are four major localization patterns of RNA molecules in mitotic cells: 1) mitotic chromosomes, 2) MiCCS, 3) mitotic cytoplasm, and 4) outer cellular membranes (Fig. 5). These localization patterns and the concentration gradients of RNA molecules would reflect the correct positioning for their function in chromosomal segregation and the formation of daughter cells. The localization patterns for 5S rRNA and 18S rRNA were mainly near the outer cellular membranes and partly through the cytoplasm, suggesting that those molecules might suit for functioning in the daughter cells such as protein synthesis. The localization patterns for ACTG and PRC1 were mainly through the cytoplasm with forming some foci, suggesting that those molecules might play crucial roles for promoting chromosome segregation during the cell division into the daughter cells.

In conclusion, future studies of the distribution of various types of RNA molecules, such as mRNA or

miRNA, would lead to the construction of global maps for the various types of RNA molecules found in the mammalian cells (Chiba and Tanabe 2009). In addition, the characterization of the distribution of RNA molecules within mitotic condensed chromosomes is the next challenge to elucidate the relationships between the structure of mitotic chromosomes and the functions of these RNA molecules.

Acknowledgments

This study was supported by a grant from Research Fellowships of the Japan Society for the Promotion of Science for Young Scientists. This study was also supported by Grants-in-aid for Scientific Research of Priority Areas from the Ministry of Education, Culture, Sports, Science, and Technology, Japan and the Center for the Promotion of Integrated Sciences (previously Hayama Center for Advanced Studies), Sokendai.

References

Azzalin CM, Reichenbach P, Khoriauli L, Giulotto E, Lingner J (2007) Telomeric repeat containing RNA and RNA surveillance factors at mammalian chromosome ends. Science 318:798-801

Bradbury EM, Inglis RJ, Matthews HR, Langan TA (1974) Molecular basis of control of mitotic cell division in eukaryotes. Nature 249:553-556

Chiba M, Tanabe H (2009) Toward global mapping for the functional RNA molecules during the mitosis in mammalian cells. In: Taniguchi K, Zhang X (eds) Advances in Chromosome Sciences Vol. 3. PAD Planning Co. Ltd., Hiroshima, pp. 157-158

Chen D, Dundr M, Wang C, Leung A, Lamond A, Misteli T, Huang S (2005) Condensed mitotic chromatin is accessible to transcription factors and chromatin structural proteins. J Cell Biol 168:41-54

Chuang P-T, Albertson DG, Meyer BJ (1994) DPY-27: a chromosome condensation protein homolog that regulates C. elegans dosage compensation through association with the X chromosome. Cell 79:459-474

Dahmus ME (1995) Phosphorylation of the C-terminal domain of RNA polymerase II. Biochem Biophys Acta 1261:171-182

Gasser S, Laroche T, Falquet J, Boy de la Tour E, Laemmli UK (1986) Metaphase chromosome structure. Involvement of topoisomerase II. J Mol Biol 188:613-629

Goldstein L (1976) Role for small nuclear RNAs in "programming" chromosomal information? Nature 261:519-521

Goldstein L, Ko C (1978) Identification of the small nuclear RNAs associated with the mitotic chromosomes of Amoeba proteus. Chromosoma 68:319-325

Gottesfeld JM, Forbes DJ (1997) Mitotic repression of the transcriptional machinery. Trends Biochem Sci 22:197-202

Gottesfeld JM, Wolf VJ, Dang T, Forbes DJ, Hartl P (1994) Mitotic repression of RNA polymerase III transcription *in vitro* mediated by phosphorylation of a TFIIIB component. Science 263:81-84

Green RJ, Bahr GF (1975) Comparison of G-, Q-, and EM-banding patterns exhibited by the chromosome complement of the Indian muntjac, *Muntiacus muntjak*, with reference to nuclear DNA content and chromatin ultrastructure. Chromosoma 50:53-67

Güttinger S, Laurell E, Kutay U (2009) Orchestrating nuclear envelope disassembly and reassembly during mitosis. Nat Rev Mol Cell Biol 10:178-191

Haugland RP (2005) A Guide to Fluorescent Probes and Labeling Technologies. In: Spence MTZ (ed) The Molecular Probes® Handbook-10th edition. Invitrogen-Molecular Probes

Hirano T, Mitchison TJ (1991) Cell cycle control of higher-order chromatin assembly around naked DNA *in vitro*. J Cell Biol 115:1479-1489

King DW, Barnhisel ML (1967) Synthesis of RNA in mammalian cells during mitosis and interphase. J Cell Biol 33:265-272

Kitagawa K, Hieter P (2001) Evolutionary conservation between budding yeast and human kinetochores. Nat Rev Mol Cell Biol 2:678-687

Kleinfeld RG, von Haam E (1959) Effect of thioacetamide on rat liver regeneration. II. Nuclear RNA in mitosis. J Biophys Biochem Cytol 6:393-398

Konrad CG (1963) Protein synthesis and RNA synthesis during mitosis in animal cells. J Cell Biol 19:267-277

Lewis C, Laemmli UK (1982) Higher order metaphase chromosome structure: evidence for

Li Q, Kim Y, Namm J, Kulkarni A, Rosania GR, Ahn YH, Chang YT (2006) RNA-selective, live cell imaging probes for studying nuclear structure and function. Chem Biol 13:615-623

Mello ML, Barbisan LF, Russo J, Vidal BC (1999) RNA relocation at mitosis in transformed and tumorigenic human breast epithelial cells. Cell Biol Int 23:125-128

Mello ML, Lareef MH, Vidal BC, Russo J (2001) RNA relocation and persistence of nucleolus-like bodies at mitosis in benzo[a]pyrene-transformed human breast epithelial cells after microcell-mediated transfer of chromosomes 11 and 17. Anal Cell Pathol 23:137-141

Prescott DM (1964) Progress in Nucleic Acid Research. In: Davidson JN, Cohn WE (eds) Academic Press, pp. 33-57

Rhee WJ, Bao G (2009) Simultaneous detection of mRNA and protein stem cell markers in live cells. BMC Biotechnol 9:30

Santangelo P, Nitin N, LaConte L, Woolums A, Bao G (2006) Live-cell characterization and analysis of a clinical isolate of bovine respiratory syncytial virus, using molecular beacons. J Virol 80:682-688

Segil N, Guermah M, Hoffmann A, Roeder RG, Heintz N (1996) Mitotic regulation of TFIID: inhibition of activator-dependent transcription and changes in subcellular localization. Genes Dev 10:2389-2400

Solovei I, Cavallo A, Schermelleh L, Jaunin F, Scasselati C, Cmarko D, Cremer C, Fakan S, Cremer T (2002a) Spatial preservation of nuclear chromatin architecture during three-dimensional fluorescence *in situ* hybridization (3D-FISH). Exp Cell Res 276:10-23

Solovei I, Walter J, Cremer M, Habermann F, Schermelleh L, Cremer T (2002b) FISH on three-dimensionally preserved nuclei. In: Squire J, Beatty B, Mai S (eds) FISH: A Practical Approach. Oxford University Press, Oxford, pp.119-157

Strunnikov AV (2005) A case of selfish nucleolar segregation. Cell Cycle 4:113-117

Tanabe H, Nakagawa Y, Minegishi D, Hashimoto K, Tanaka N, Oshimura M, Sofuni T, Mizusawa H (2000) Human monochromosome hybrid cell panel characterized by FISH in the JCRB/HSRRB. Chromosome Res 8:319-334

Uchiyama S, Kobayashi S, Takata H, Ishihara T, Hori N, Higashi T, Hayashihara K, Sone T, Higo D, Nirasawa T, Takao T, Matsunaga S, Fukui K (2005) Proteome analysis of human metaphase chromosomes. J Biol Chem 280:16994-17004

Uemura T, Ohkura H, Adachi Y, Morino K, Shiozaki K, Yanagida M (1987) DNA topoisomerase II is required for condensation and separation of mitotic chromosomes in S. pombe. Cell 50:917-925

van Holde KE (1988) Chromatin. Springer, New York

van Hooser AA, Yuh P, Heald R (2005) The perichromosomal layer. Chromosoma 114:377-388

Ved Brat S, Verma RS, Dosik H (1979) Structural organization of chromosomes of the Indian muntjac (*Muntiacus muntjak*). Cytogenet Cell Genet 24:201-208

Wieland G, Orthaus S, Ohndorf S, Diekmann S, Hemmerich P (2004) Functional complementation of human centromere protein A (CENP-A) by Cse4p from Saccharomyces cerevisiae. Mol Cell Biol 24:6620-6630

Wong LH, Brettingham-Moore KH, Chan L, Quach JM, Anderson MA, Northrop EL, Hannan R, Saffery R, Shaw ML, Williams E, Choo KH (2007) Centromere RNA is a key component for the assembly of nucleoproteins at the nucleolus and centromere. Genome Res 17:1146-1160